Appl. Math. Mech. -Engl. Ed., **35**(2), 229–236 (2014)
DOI 10.1007/s10483-014-1786-6

Applied Mathematics and Mechanics (English Edition)

Nonlinear characteristics of circular-cylinder piezoelectric power harvester near resonance based on flow-induced flexural vibration mode*

Hai-ren WANG (王海仁)[1,2], Jie-min XIE (谢捷敏)[2], Xuan XIE (谢 旋)[2], Yuan-tai HU (胡元太)[2], Ji WANG (王 骥)[3]

(1. Purple Mountain Observatory, Chinese Academy of Sciences, Nanjing 210008, P. R. China;
2. Department of Mechanics, Huazhong University of Science and Technology, Wuhan 430074, P. R. China;
3. Piezoelectric Device Laboratory, Department of Mechanics and Engineering Science, School of Mechanical Engineering and Mechanics, Ningbo University, Ningbo 315211, Zhejiang Province, P. R. China)

Abstract The nonlinear behaviors of a circular-cylinder piezoelectric power harvester (CCPPH) near resonance are analyzed based on the flow-induced flexural vibration mode. The geometrically-nonlinear effect of the cylinder is studied with considering the in-plane extension incidental to the large deflection. The boundary electric charges generated from two deformation modes, flexure and in-plane extension, were distinguished with each other because the charge corresponding to the latter mode produces no contribution to the output current. Numerical results on output powers show that there are multi-valuedness and jump behaviors.

Key words piezoelectric power harvester, nonlinear behavior, large deflection, in-plane extension, multivaluedness

Chinese Library Classification O175.13
2010 Mathematics Subject Classification 70K20

1 Introduction

Recently, the wireless electronic devices (WEDs), which have developed rapidly, have been widely used in many fields. Providing WEDs with energy without a wired power source is an interesting issue. Harvesting energy from the surrounding environment is an effective way[1]. Owing to the strong electromechanical coupling property, piezoelectric materials are used to manufacture high-performance piezoelectric power harvesters that are good at scavenging energy from mechanical vibrations[1–4].

This paper is concerned with the converting mechanical energy from flow-induced vibrations into electric energy. Piezoelectric power harvesters that are composed of flexible piezoelectric

* Received Feb. 27, 2013 / Revised Aug. 20, 2013
Project supported by the National Natural Science Foundation of China (Nos. 10932004 and 11272127) and a grant from the Impact and Safety of Coastal Engineering Initiative, a Center of Excellence Program of Zhejiang Provincial Government at Ningbo University (No. zj1213)
Corresponding author Yuan-tai HU, Professor, Ph. D., E-mail: hudeng@263.net

films or strips are used for this purpose[5–8]. These harvesters are fitted behind a blunt body in a flow from which the asymmetric vortex sheds, as excites the harvesters into transversal vibrations. Due to the transversal vibration, an electrical output voltage is generated. Resorting to the theory of linear piezoelectricity, the basic performances of the piezoelectric devices can be conducted[4–9]. To extract energy as much as possible, the harvesters are usually designed as resonant devices operating near resonance. There are some nonlinear effects responsible for some behaviors such as jump and multivaluedness under that situation. Obviously, these nonlinear behaviors, e.g., multivaluedness and jump phenomena, which are usually considered undesirable, are to be avoided in design. A nonlinear analysis is necessary for the purpose of determining the linear operating range of the devices. Recently, Hu et al.[10] analyzed the nonlinear performance of a piezoelectric power harvester consisting of a mass and a plate in thickness-shear vibration. Xue and Hu[11] analyzed the geometrically nonlinear characteristics of a harvester consisting of circular piezoelectric plate by axially symmetrical vibration mode. In this paper, we study a circular-cylinder piezoelectric power harvester (CCPPH) based on the flow-induced flexural vibration mode. The resonant frequency range of the CCPPH is considered to be relatively low in deflection mode. Therefore, the energy-scavenging structure usually resonates easily with ambient vibrations[12–13]. Therefore, we study the nonlinear characteristics of the harvester, taking into account the in-plane extension incidental to large transversal deflection. In Section 2, we establish the motion equations of the CCPPH near resonance with flow-induced flexural vibration mode. Because the polarization charges generated by the in-plane extension deformation produce no effect to the output current, the boundary electric charges are carefully divided into two parts according to the different deformation modes. After re-establishing the relationship between output current and boundary electric charges, a lot of computations on output powers are conducted. Numerical results are shown in Section 3, and some conclusions are drawn in Section 4.

2 Analysis of CCPPH with geometrical nonlinearity

The structure of a CCPPH is shown in Fig. 1, where the flow is along the x_3-direction to induce the beam flexurally vibrating in the x_1x_2-plane. For the tube, $L \gg d \gg h$, the length is $2L$, the diameter is $d = 2R$, and the thickness is h. The electrodes of the CCPPH cover its whole length with the electrode configuration at the cross section shown in Fig. 1(b). The whole inner surface is regarded as an electrode that is grounded. The top of the outer surface is designed as an electrode. Like the top, the bottom has a similar electrode. Both the top electrode and the bottom electrode sweep out an equal angle that is 2α. α cannot be larger than $\pi/2$ for the purpose of avoiding the overlap between the top electrode and the bottom electrode. The CCPPH is poled along the R-direction. The output voltage between the top electrode and the bottom electrode is regarded as $2V$, which loads on an resistance Z. Considering that the two ends $x_1 = \pm L$ are simply-supported, it is not allowable to occur any in-plane displacements $u_1 = \pm L$.

When the energy-scavenging structure is driven by the flow vortex shedding into flexural vibration near resonance, large deflection induces an incidental in-plane extension together with an axial force N in the x_1-direction[14]. Then, an additional electric-potential difference V_0 between the outer and the central electrodes is excited by the in-plane extension with appearance of the corresponding electric charge Q_0 at the top/bottom of the tube. Both flexural motion of the CCPPH in the x_2-direction with the deflection $u_2(x_1, t)$ and extension motion in the x_1-direction with the extension $u_1(x_1, t)$ are considered. Thus, the in-plane normal strain for the beam can be written as[15–16]

$$S_1 = u_{1,1} + \frac{1}{2}(u_{2,1})^2 - x_2 u_{2,11}. \tag{1}$$

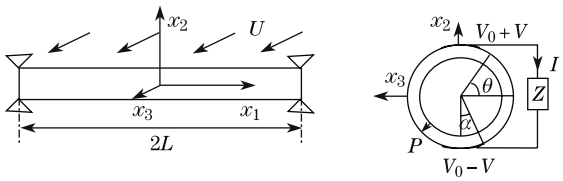

(a) Side section (b) Cross section

Fig. 1 Structure of CCPPH

According to the electrodes shown in Fig. 1(b), the electric voltage can be written as

$$\begin{cases} V_1 = V_0 + V, & \dfrac{\pi}{2} - \alpha < \theta < \dfrac{\pi}{2} + \alpha, \\ V_2 = V_0 - V, & \dfrac{3}{2}\pi - \alpha < \theta < \dfrac{3}{2}\pi + \alpha, \end{cases} \tag{2}$$

where V stands for the electric-potential difference between the outer and the central electrodes generated by the deflection, and V_0 is the electric-potential difference generated by the in-plane extension. The electric field can be written as

$$E_r = \begin{cases} -\dfrac{V_0 + V}{h}, & \dfrac{\pi}{2} - \alpha < \theta < \dfrac{\pi}{2} + \alpha, \\ \dfrac{-V_0 + V}{h}, & \dfrac{3}{2}\pi - \alpha < \theta < \dfrac{3}{2}\pi + \alpha. \end{cases} \tag{3}$$

The constitutive relations of the CCPPH can be written as[8]

$$\begin{cases} T_1 = s_{11}^{-1} u_{1,1} + s_{11}^{-1} (u_{2,1})^2/2 - s_{11}^{-1} x_2 u_{2,11}^{-} s_{11}^{-1} d_{31} E_r, \\ D_r = s_{11}^{-1} d_{31} u_{1,1} + s_{11}^{-1} d_{31} (u_{2,1})^2/2 - s_{11}^{-1} d_{31} x_2 u_{2,11}^{+} \bar{\varepsilon}_{33} E_r, \end{cases} \tag{4}$$

where T_1 and D_r stand for the stress and the electric displacement. d_{31}, ε_{33}, and s_{11} are the piezoelectric coefficient constant, the dielectric constant, and the elastic compliance constant, respectively. In the above, we have denoted that $\bar{\varepsilon}_{33} = \varepsilon_{33}(1 - k_{31}^2)$ and $k_{31}^2 = d_{31}^2/(\varepsilon_{33} s_{11})$. An axial force N corresponding to the in-plane extension can be obtained using the expression for T_1 in (4) as

$$N = \int_s T_1 \mathrm{d}A = \pi R h s_{11}^{-1} (2u_{1,1} + (u_{2,1})^2) + 4\alpha R V_0 s_{11}^{-1} d_{31}. \tag{5}$$

Taking an integral at N along the tube length leads to

$$\int_{-L}^{L} N \mathrm{d}x_1 = \overline{N} \cdot 2L = \frac{EI}{R^2} \int_{-L}^{L} (u_{2,1})^2 \mathrm{d}x_1 + 4\alpha R V_0 s_{11}^{-1} d_{31} \cdot 2L. \tag{6}$$

We therefore obtain the average axial force $\overline{N}$ as

$$\overline{N} = \frac{EI}{2R^2 L} \int_{-L}^{L} (u_{2,1})^2 \mathrm{d}x_1 + 4\alpha R V_0 s_{11}^{-1} d_{31}. \tag{7}$$

The bending moment M can be obtained by using the expression for T_1 in (4) as

$$M = \int_S x_2 T_1 \mathrm{d}A = -EI u_{2,11} + s_{11}^{-1} d_{31} V 4R^2 \sin\alpha. \tag{8}$$

The dynamic effect in the x_2-direction is much stronger than that in the x_1-direction. Hence, the latter can be reasonably ignored for simplicity, and thus, the motion equation in the x_1-direction reduces to an equilibrium condition. Under this case, the axial force N can be approximately replaced by $\overline{N}$. The motion equation of a beam in the x_2-direction can be written as[16]

$$M_{,11} + (\overline{N}u_{2,1})_{,1} + F(x_1, t) - m\ddot{u}_2 = 0, \tag{9}$$

where $m = 2\pi\rho Rh$ stands for the mass per unit length of the CCPPH. $F(x_1, t)$ stands for the load per unit length acted at the CCPPH. Substituting (8) into (9), we obtain

$$-EIu_{2,1111} + \overline{N}u_{2,11} + F(x_1, t) = m\ddot{u}_2. \tag{10}$$

For a simply-supported beam, we have the boundary conditions for $u_2(x_1, t)$ as

$$u_2(-L, t) = u_2(L, t) = 0, \quad M(-L, t) = M(L, t) = 0. \tag{11}$$

From Ref. [14], the flow load on the CCPPH is independent of x_1 and can be written as

$$F(t) = f\exp(\mathrm{i}\omega t) = 0.5\rho_L U^2 C_{L0} d\sin\omega t, \tag{12}$$

where f, ρ_L, U, and C_{L0} are the load amplitude, the fluid density, the speed of the flow, and a known constant, respectively. Using the Galerkin method, we approximately write $u_2(x_1, t)$ as follows:

$$u_2(x_1, t) = 2(h + R)(\psi(t)(1 - \xi^2) + \phi(t)(1 - \xi^2)^2), \quad \xi = \frac{x_1}{L}, \tag{13}$$

which satisfies the boundary condition (11) in advance[11]. From (13) and (11), we have

$$\psi(t) = 4\varphi(t) + KV, \quad K = -\frac{d_{31}L^2R^2\sin\alpha}{EIs_{11}(h + R)}.$$

Taking an integral at (4) on the cross section of the beam yields

$$V_0 = A\psi^2 + B\phi\psi + C\phi^2, \tag{14}$$

where

$$\begin{cases} A = -280\gamma(3h\pi R^3 - EIs_{11}), \quad B = 448EI\gamma s_{11}, \\ C = 256EI\gamma s_{11}, \quad \gamma = \dfrac{(h + R)^2}{105d_{31}L^2R^3(\pi - 2\alpha)}. \end{cases}$$

Applying the Galerkin technique to (10) yields

$$\int_{-L}^{L} (-EIu_{2,1111} + Nu_{2,11} + F(x_1, t) - m\ddot{u}_2)u_2 \mathrm{d}x_1 = 0. \tag{15}$$

Furthermore, we obtain the governing equation for $\varphi(t)$ as follows:

$$\ddot{\phi}(t) + c_1\phi(t) + c_2\phi^3(t) + c_3V = F\sin\omega t, \tag{16}$$

where

$$\begin{cases} c_1 = \dfrac{6.10EI}{mL^4}, \quad c_2 = \dfrac{51.71hR^3\varsigma}{L^4ms_{11}(\pi - 2\alpha)}, \\ c_3 = \dfrac{1.27EIK}{mL^4}, \quad F = \dfrac{0.13f}{m(h + R)}, \quad \varsigma = 17\pi - 70\alpha. \end{cases}$$

The electric charges at the top and bottom electrodes are

$$\begin{cases} Q_1 = Q_0 + Q_{\rm e}, & \dfrac{\pi}{2} - \alpha < \theta < \dfrac{\pi}{2} + \alpha, \\ Q_2 = Q_0 - Q_{\rm e}, & \dfrac{3}{2}\pi - \alpha < \theta < \dfrac{3}{2}\pi + \alpha. \end{cases} \tag{17}$$

It is well-known that no current presents for the piezoceramic tube subjected to in-plane deformation only because there does not exist any electric difference between the two outer electrodes under that situation. Thus, the output current flowing out from the top to the bottom electrode would be obtained from

$$I = -\frac{1}{2}(\dot{Q}_1 - \dot{Q}_2) = -\dot{Q}_{\rm e} \tag{18}$$

with the electric charge $Q_{\rm e}$ decided by

$$\begin{aligned} Q_{\rm e} &= -\int_{-L}^{L} {\rm d}x_1 \int_{\pi/2-\alpha}^{\pi/2+\alpha} (D_r|_{x_2=R} - D_r|_{x_2=-R}) R {\rm d}\theta \\ &= 4R^2 s_{11}^{-1} d_{31} u_{2,1}(L,t) \sin\alpha + \frac{4}{h}\alpha\bar{\varepsilon}_{33} RL(V_0 + V). \end{aligned} \tag{19}$$

We note from (18) and (19) that V_0 has influence on the output current. This is easily understood because the electric-field generated by V_0 still produces driving effect on the boundary electric charge $Q_{\rm e}$. In the external circuit, V and I are related through the Ohm law

$$I = 2\frac{V}{Z}. \tag{20}$$

Substituting (18) and (19) into (20), we get

$$-4R^2 s_{11}^{-1} d_{31} \dot{u}_{2,1}(L,t) \sin\alpha - \frac{4}{h}\alpha\bar{\varepsilon}_{33} RL(\dot{V}_0 + \dot{V}) = 2\frac{V}{Z}. \tag{21}$$

Further, we obtain the following equation for the output voltage from (13) and (21):

$$\dot{V} + k_1 V + k_2 \phi\dot{\phi} + k_3\dot{\phi} = 0, \tag{22}$$

where

$$\begin{cases} \vartheta = \pi s_{11}\alpha\bar{\varepsilon}_{33} + 4d_{31}^2 \sin^2\alpha, \quad k_1 = \dfrac{h\pi s_{11}}{2LRZ\vartheta}, \\ k_2 = \dfrac{216.62}{d_{31}L^2(\pi - 2\alpha)\vartheta} h(h+R)^2 s_{11}\alpha\bar{\varepsilon}_{33}, \\ k_3 = -\dfrac{16}{L^2\vartheta} d_{31} h\pi R(h+R)\sin\alpha. \end{cases}$$

Let

$$\varphi(t) = U_1 \sin\omega t + U_2 \cos\omega t, \tag{23}$$

where U_1 and U_2 are undetermined constants. Then, we obtain

$$V = -k_3\varphi + H_1 \sin\omega t + H_2 \cos\omega t + H_3 \sin 2\omega t + H_4 \cos 2\omega t. \tag{24}$$

where

$$\begin{cases} H_1 = -\dfrac{k_3}{k_1^2+\omega^2}(-k_1^2U_1 - k_1\omega U_2), \\ H_2 = -\dfrac{k_3}{k_1^2+\omega^2}(k_1\omega U_1 - k_1^2U_2), \\ H_3 = -\dfrac{k_2\omega}{2(k_1^2+4\omega^2)}(k_1(U_1^2-U_2^2) + 4U_1U_2\omega), \\ H_4 = -\dfrac{k_2\omega}{2(k_1^2+4\omega^2)}(k_1U_1U_2 - \omega(U_1^2-U_2^2)). \end{cases} \tag{25}$$

We substitute (23) and (24) into (16), collect both the sine and cosine term coefficients, respectively, and neglect the higher-order terms[10–11]. Then, we obtain

$$\begin{cases} 0.75c_2U_1^3 + (\omega_0^2-\omega^2)U_1 + 0.75c_2U_1U_2^2 + c_3H_1 - F = 0, \\ 0.75c_2U_2^3 + (\omega_0^2-\omega^2)U_2 + 0.75c_2U_2U_1^2 + c_3H_2 = 0, \end{cases} \tag{26}$$

where $\omega_0^2 = c_1 - c_3k_3$, and ω_0 is the resonant frequency of harvester. Equation (26) can be solved numerically. Therefore, we can get U_1 and U_2. $\varphi(t)$ and V can be obtained from (23) and (24). The output power P can be given as

$$P = \frac{\omega}{2\pi}\int_t^{t+2\pi/\omega} 2IV\,\mathrm{d}t. \tag{27}$$

3 Numerical results and discussion

In this section, the numerical results of CCPPH are presented. In the calculations, we consider CCPPH of polarized ceramics PZT-5H with $\rho = 7\,500\,\mathrm{kg/m^3}$ and[17]

$$\begin{cases} s_{11} = 16.5, \quad s_{33} = 20.7, \quad s_{44} = 43.5, \quad s_{12} = -4.78, \quad s_{13} = -8.45\times10^{-12}\,\mathrm{m^2/N}, \\ d_{31} = -274, \quad d_{15} = 741, \quad d_{33} = 593\times10^{-12}\,\mathrm{C/N}, \\ \varepsilon_{11} = 3\,130\varepsilon_0, \quad \varepsilon_{33} = 3\,400\varepsilon_0, \quad \varepsilon_0 = 8.854\times10^{-12}\,\mathrm{F/m}. \end{cases} \tag{28}$$

The geometric parameters of the tube are $d = 2R = 10\,\mathrm{mm}$, $h = 0.5\,\mathrm{mm}$, $2L = 200\,\mathrm{mm}$, and $\alpha = 60^\circ$ unless stated otherwise. In addition, we denote $\Delta\omega = \omega - \omega_0$, where $\omega_0 = 2\,330\,\mathrm{rad/s}$. For the fluid, we consider air at 20°C with the density $\rho_L = 1.204\,7\,\mathrm{kg/m^3}$. The air viscosity $\mu = 1.81\times10^{-5}\,\mathrm{N\cdot sm^{-2}}$, and other related parameters are $\nu = \frac{\mu}{\rho_L} = 1.502\,4\times10^{-5}\,\mathrm{m^2\cdot s^{-1}}$, $C_{L0} = 0.63$, and $U = \frac{d}{k}\omega$, where $k = 1.2$[14]. We choose $Z = 1\,000\,\mathrm{K\Omega}$ unless stated otherwise.

Figures 2 and 3 show the dependence of P upon $\Delta\omega$ for different tube diameters and different resistances. At the left of resonance, output power is multivalued with jump. Thus, we should design CCPPH structure to operate on the right side adjacent to the resonance to avoid the multivaluedness and jump, otherwise, output power of CCPPH will be either very low or unstable. From Fig. 2, we can also find that the location of jump moves left and the graph of P-$\Delta\omega$ becomes vertical gradually with the increase in the tube diameter. This is understandable because the increase in the tube diameter makes the energy-scavenging structure tend to a linear resonance from a nonlinear resonance. Figure 3 shows the influence of impedance on output power with $d = 10\,\mathrm{mm}$. The magnitude of output power decreases when impedance

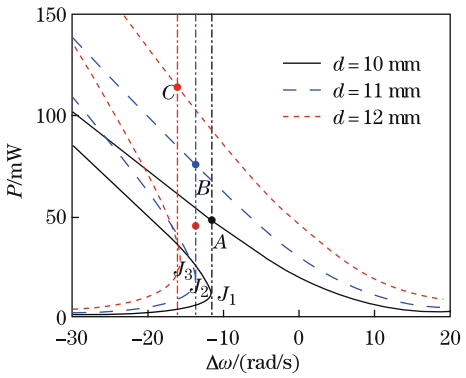

Fig. 2 Dependence of P upon $\Delta\omega$ for different tube diameters

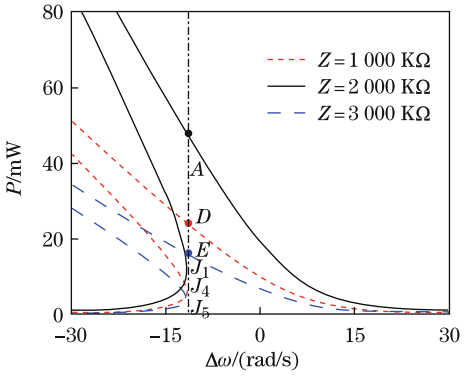

Fig. 3 Dependence of P upon $\Delta\omega$ for different resistances

increases. However, the location of jump has less dependence on impedance. This indicates that the range of nonlinear region is independent of external-circuit.

Figure 4 shows the dependence of output power upon the tube diameter for different electric resistances with $\Delta\omega = -20\,\mathrm{rad/s}$. After the tube diameter is designed at the right of FGHK, multi-valuedness disappears and the energy-scavenging structure gets a relatively large output power. The same as above, external resistance does not influence the location of FGHK although it produces large effect on the output power magnitude.

To further realize the multivaluedness and jumps of a power harvester near resonance, we calculate the dependence of P upon the tube diameter d for different $\Delta\omega$ in Fig. 5. Numerical results show that a larger value of $|\Delta\omega|$ corresponds to a larger nonlinear P-d loop. When $|\Delta\omega|$ decreases, the P-d loop reduces, too, and gradually shrinks to a point which implies a linear resonance as discussed in Fig. 2.

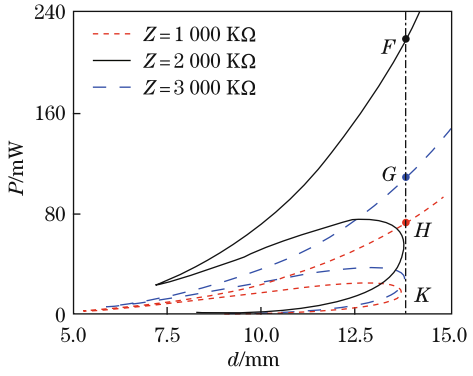

Fig. 4 Dependence of P upon d for different resistances with $\Delta\omega = -20\,\mathrm{rad/s}$

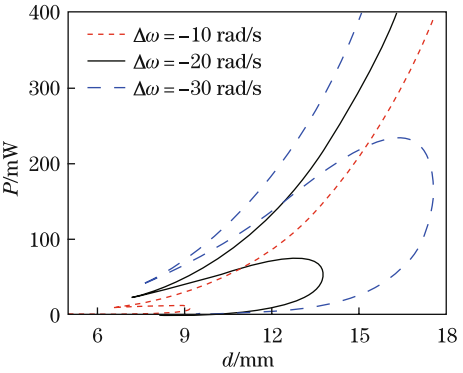

Fig. 5 Dependence of P upon d for different $\Delta\omega$

4 Conclusions

The nonlinear performance of CCPPH near resonance is presented with consideration of in-plane extension induced by large deflection. The boundary electric charges corresponding to two deformation modes, deflection and in-plane extension, are distinguished with each other.

Basic nonlinear behaviors of the harvesting structure near resonance are predicted. The multi-valuedness and jump phenomena is shown by numerical results, which are useful in CCPPH design.

Acknowledgements The authors would like to thank Professor Jia-shi YANG at University of Nebraska for helpful discussion.

References

[1] Roundy, S., Wright, P. K., and Rabaey, J. A study of low level vibrations as a power source for wireless sensor nodes. *Computer Communications*, **26**, 1131–1144 (2003)

[2] Cho, Y. S., Pak, Y. E., Han, C. S., and Ha, S. K. Fiver-port equivalent electric circuit of piezoelectric bimorph beam. *Sensors and Actuators*, **84**, 140–148 (2000)

[3] Jiang, S. N. and Hu, Y. T. Analysis of a piezoelectric bimorph plate with a central-attached mass as an energy harvester. *IEEE Transactions on Ultrasonics, Ferroelectrics, and Frequency Control*, **54**, 1463–1469 (2007)

[4] Jiang, S. N., Li, X. F., Guo, S. H., Hu, Y. T., Yang, J. S., and Jiang, Q. Performance of a piezoelectric bimorph for scavenging vibration energy. *Smart Materials and Structures*, **14**, 769–774 (2005)

[5] Allen, J. J. and Smits, A. J. Energy harvesting eel. *Journal of Fluids and Structures*, **15**, 629–640 (2001)

[6] Carroll, C. B. *Energy Harvesting Eel*, United States Patent, Patent No. US-6424079-B1 (2002)

[7] Akaydin, H. D., Elvin, N., and Andreopoulos, Y. Energy harvesting from highly unsteady fluid flows using piezoelectric materials. *Journal of Intelligent Material Systems and Structures*, **21**, 1263–1278 (2010)

[8] Xie, J. M., Yang, J. S., Hu, H. P., Hu, Y. T., and Chen, X. D. A piezoelectric energy harvester based on flow-induced flexural vibration of a circular cylinder. *Journal of Intelligent Material Systems and Structures*, **23**, 135–139 (2011)

[9] Yang, J. S., Zhou, H. G., Hu, Y. T., and Jiang, Q. Performance of a piezoelectric harvester in thickness-stretch mode of a plate. *IEEE Transactions on Ultrasonics, Ferroelectrics, and Frequency Control*, **52**, 1872–1876 (2005)

[10] Hu, Y. T., Xue, H., Yang, J. S., and Jiang, Q. A Nonlinear behavior of a piezoelectric power harvester near resonance. *IEEE Transactions on Ultrasonics, Ferroelectrics, and Frequency Control*, **53**, 1387–1391 (2006)

[11] Xue, H. and Hu, H. P. Nonlinear characteristics of a circular plate piezoelectric harvester with relatively large deflection near resonance. *IEEE Transactions on Ultrasonics, Ferroelectrics, and Frequency Control*, **55**, 2092–2096 (2008)

[12] Kim, S., Clark, W. W., and Wang, Q. M. Piezoelectric energy harvesting with a clamped circular plate: analysis. *Journal of Intelligent Material Systems and Structures*, **16**, 847–854 (2005)

[13] Kim, S., Clark, W. W., and Wang, Q. M. Piezoelectric energy harvesting with a clamped circular plate: experimental study. *Journal of Intelligent Material Systems and Structures*, **16**, 855–863 (2005)

[14] Fung, Y. C. Some aemoelastic problems in civil and mechanical engineering. *An Introduction to the Theory of Aeroelasticity*, Dover Publications Inc., New York (1969)

[15] Eisley, J. G. Nonlinear vibration of beams and rectangular plates. *Zeitschrift für Angewandte Mathematik und Physik*, **15**, 167–175 (1964)

[16] Pirbodaghi, T., Fesanghary, M., and Ahmadian, M. T. Non-linear vibration analysis of laminated composite plates resting on non-linear elastic foundations. *Journal of the Franklin Institute*, **348**, 353–368 (2011)

[17] Auld, B. A. Properties of materials. *Acoustic Fields and Waves in Solids*, John Wiley & Sons Inc., New York (1973)